Journal of Analytical and Applied Pyrolysis 192 (2025) 107289

Contents lists available at ScienceDirect

Journal of Analytical and Applied Pyrolysis

journal homepage: www.elsevier.com/locate/jaap

High-temperature pyrolysis of low-density polyethylene for hydrogen production and carbon capture

Cedric Karel Fonzeu Monguen [1], Ahmet Çelik [1], Felix Straub, Vanessa Maria Pohl, Jannis Kühn, Patrick Lott, Olaf Deutschmann [*]

Institute for Chemical Technology and Polymer Chemistry (ITCP), Karlsruhe Institute of Technology (KIT), Engesserstr. 20, Karlsruhe 76131, Germany

A R T I C L E I N F O

Keywords:
LDPE
Non-catalytic pyrolysis
Hydrogen yield
Decarbonization
Solid carbon

A B S T R A C T

Utilizing low-density polyethylene (LDPE) as a feedstock, non-catalytic thermal pyrolysis represents a promising technology for large-scale hydrogen generation and carbon capture. Furthermore, the use of the solid carbon byproduct generated during the process, enhances the operation's economic feasibility. This work uses the model compound to reveal the potential of LDPE pyrolysis for producing hydrogen and capturing carbon. A laboratory-scale high-temperature fixed bed reactor is operated in the temperature ranging from 700 °C to 1600 °C, with LDPE pellets of 5 mm in diameter. Despite a decrease in gas yield to 13.7 wt% as the temperature increases, the hydrogen yield significantly increased up to 11.0 wt% from 900 °C to 1600 °C. Approximately two-thirds of the hydrogen present in the polymer was identified as molecular hydrogen in the product gas. At 1600 °C, a purity of 98.5 mol% was achieved for the hydrogen produced, while the product gas at temperatures ranging from 700 °C to 900 °C predominantly contained methane and ethylene. The analysis of the influence of temperature on the condensable product phase demonstrated an increase in the yields of aliphatic and polycyclic aromatic hydrocarbons (PAHs) species up to a temperature of 1000 °C. The decrease in yield of Aliphatic and PAHs from 1000 °C onwards could be attributed to the gradual decarbonization of the gas phase through the formation of solid carbon. Additionally, the produced solid carbon was analyzed using various techniques, including TEM, SEM, DLS, TGA, XRD, and Raman spectroscopy. The results demonstrated its potential as a sustainable industrial carbon material.

1. Introduction

Low and high-density polyethylene (LDPE, HDPE), polypropylene (PP), polystyrene (PS), polyvinyl chloride (PVC), and polyethylene terephthalate (PET) are the most commonly utilized plastics in everyday life and industry [1]. Polyethylene (PE) including LDPE and HDPE, is the most widely manufactured and consumed plastic globally, accounting for 32 % of the overall composition of municipal solid waste [2]. LDPE is often used in applications such as blister packages, drug packaging, and films due to its durability and flexibility [3]. LDPE's crystalline structure is less efficient in chain packing due to significant short and long-chain branching [2]. HDPE is a thermoplastic renowned for its impressive strength-to-density ratio, and therefore, it finds wide application in the production of detergent bottles, food packaging, as well as agricultural films [4]. To date, over 70 % of plastic waste (PW) is either landfilled or improperly discarded worldwide [5], which commonly results in an accumulation of PW that raises environmental concerns, in particular, due to toxic additives in ancient plastics, the prevalence of marine microplastics, and the unlawful dumping of PW [6,7]. To address this issue, researchers have explored various ways to convert PW into highly profitable products. Although in this context especially incineration and mechanical recycling have been identified as potential solutions, incineration results in the emission of toxic gases such as NO_x, N_2O, and CO, and thus contribute to air pollution. Furthermore, both methods can be expensive and not economically feasible in certain situations. Therefore, developing novel approaches to overcome these problems is crucial.

Chemical recycling has been considered as a potential solution for various polymers, including those that cannot be mechanically recycled [8,9]. Within the several chemical recycling approaches, pyrolysis stands out as an appealing alternative for converting PW into more useful products such as gas fuel, fuel oil, or raw materials for the

* Corresponding author.
E-mail address: deutschmann@kit.edu (O. Deutschmann).
[1] *Both contributed equally*

https://doi.org/10.1016/j.jaap.2025.107289
Received 24 April 2025; Received in revised form 20 June 2025; Accepted 13 July 2025
Available online 14 July 2025

chemical industry [10,11]. Pyrolysis is a thermochemical process that involves the degradation of (organic) material through heating in a commonly oxygen-free atmosphere. One important product of this process is hydrogen, which has gained significant interest because it is a comparably versatile carbon-free energy carrier [12,13]. Hydrogen is widely employed in various industrial applications, including ammonia and methanol production, electricity generation, and fuel production [14,15]. Presently, the majority of hydrogen is generated from fossil fuels via natural gas (methane) steam reforming, which commonly employs the utilization of nickel-based catalysts at high temperatures (700 °C - 1000 °C) and pressures (0.3 MPa - 2.5 MPa) [16]. Obtaining hydrogen from PW instead not only provides an alternative raw material but particularly addresses the environmental challenges associated with managing PW.

Moreover, previous studies highlighted the significance of thermal pyrolysis process for plastic wastes in comparison to mechanical recycling and landfilling. H. Almohamadi et al. [17] demonstrated that, using an Aspen Plus model, a hydrogen yield of 70–85 mol% results in a minimum selling price (MSP) ranging from 0.10 to 0.09 €/kg. According to Volk et al. [18], in the context of Germany, thermal pyrolysis of 1 kg of input plastic waste generates a global warming potential (GWP) of 0.99 $kgCO_2e/kg$, a cumulative energy demand (CED) of 14.99 MJ/kg, a product cost of 0.24 €/kg, and a carbon efficiency of 59 %, while mechanical recycling exhibits a GWP of 0.67 $kgCO_2e/kg$, a CED of 3.83 MJ/kg, a product cost of 0.10 €/kg, and a carbon efficiency of 20 %. In the case of the United States. Salahuddin et al. [19] found that thermal pyrolysis yields a positive profit (~ 21.59 €/ton) and high efficiency (70 %) compared to landfill (5 %, −43.18 €/ton) and mechanical recycling (66 %, −133.13 €/ton), confirming its economic viability for plastic waste management. However, it is crucial to maximize their profitability by enhancing system effectiveness, and reducing energy and material usage because this process could take 5–10 years to become profitable, which is generally considered long for investors.

Several groups have extensively investigated the pyrolysis of polyethylene. Kaminsky et al. [20] carried out research on polyethylene pyrolysis at various temperatures. Williams et al. [21] explored the role of temperature during the pyrolysis of LDPE in a fluidized bed reactor. Similarly, Milne et al. [22] studied the pyrolysis of LDPE in a pilot plant scale internally circulating fluidized bed (ICFB) reactor, examining the impact of temperature and residence time on the composition of the pyrolysis gas. Lopez et al. [23] revealed that the overall yield of gas and liquid reached up to 65 % if PE waste is pyrolyzed at 480 °C. In another study by Sogancioglu et al. [2], a gas yield of 11.49 % was achieved at 300 °C and increased to 20.71 % at 700 °C. Regarding hydrogen content, Honus et al. [24] report 18 % of H_2 at 500 °C, which decreases to 14 % at 900 °C. While numerous of these studies have acknowledged the impact of temperature and residence time on product composition, the specific effect of temperature on hydrogen production has not been clearly explained in the literature, with different authors obtaining contradictory results. Moreover, most researchers have focused on temperatures ranging from 300 °C to 700 °C. Additionally, the influence of temperature on condensed phase products as well as on solid carbon formation have not been sufficiently examined during the thermal pyrolysis of PW. Furthermore, although heterogeneous catalysts such as Fe_2O_3 [25], $Ca(OH)_2$ [25], Al_2O_3 [26], natural and synthetic zeolite [23,27] are effective in reducing the heat required for waste plastics decomposition, particularly due to their ability to remove tar, and produce high yields of syngas, they are prone to rapid deactivation due to coking and could potentially contaminate the carbon product that might be used as C-source in a variety of applications [11].

Based on the aforementioned observations, a non-catalytic thermal pyrolysis approach is proposed for low-density polyethylene decomposition to H_2 and solid carbon at temperatures ranging from 700 °C to 1600 °C. Here, a lab-scale high-temperature reactor filled with LDPE pellets is used and operated at a pressure of 1 bar.

2. Experimental

2.1. Feedstock

A commercially available low-density polyethylene, denoted LDPE (linear formula: $H(CH_2CH_2)_nH$, product number 428043), in the form of pellets (granule size of 5 mm with smooth surface) was obtained from Sigma-Aldrich (affiliates of Merck KGaA, Darmstadt, Germany). The properties of the LDPE are: density of 0.925 g mL^{-1}, the melt index of 2.5 g min^{-1} (190 °C /2.16 kg), melting point of 116 °C, and transition temperature of 93 °C.

2.2. LDPE pellets and solid carbon characterization

The LDPE sample and the solid carbon produced were subject to thermogravimetric analysis (TGA) in an STA 409 C/CD device (NETZSCH, Karlsruhe, Germany) to study their thermal stability. For this, 20.0 mg of LDPE pellets were placed in a ceramic crucible and heated from 20 °C to 600 °C (by 10 °C min^{-1}) in N_2 atmosphere with a total flow rate of 65.0 mL min^{-1}. Figure S1 in the supplementary information (SI) shows the TGA results on the LDPE pellets. To analyze the structural properties and defects, Raman spectra of the soot particles were recorded with a Renishaw Model inVia Reflex Raman spectrometer, covering the range of 200–2000 cm^{-1} using a 525.0 nm laser at room temperature. Dynamic Light Scattering (DLS) was conducted in a Zetasizer nano by Malvern Pananalytical instrument to provide the particle size distributions. Scanning electron microscopy (SEM) and transmission electron microscopy (TEM) was performed in Quanta 200 FEI microscope with an accelerating voltage of 8–10 kV and Thermis Z microscope from ThermoFischer at an electron acceleration voltage of 300 kV, respectively, to offer insights into surface morphology and internal structure of the solid carbon samples. To analyze the microscopy images, the particle diameters were measured using the ImageJ program. This involved comparing the diameter to a pixel scale. A total of 200 particles were randomly recorded from the different TEM images and a mean diameter was calculated. Figure S2 in SI illustrates an example of these measurements. X-ray diffraction (XRD) patterns were obtained using a Malvern Pananalytical Xpert pro instrument with Cu Kα radiation, scanning from 5.0° to 90.0°, to reveal crystallographic properties.

2.3. Pyrolysis experiment

The pyrolysis experiments were conducted in the same high-temperature flow reactor previously described in our previous publications [28–30] and which was modified to enable plastic pyrolysis experiments, as schematically shown in Fig. 1a. The setup consists of a gas supply system, a tubular reactor in laminar-flow geometry, an analytic gas and exhaust gas section. The reaction gas stream enters an electrically heated Al_2O_3-based ceramic reactor tube (DEGUSSIT AL23 by Friatec/Aliaxis) with an inner diameter of 20 mm. To ensure efficient insulation and safe reactor operation, even in the case of over-pressure in the reactor tube, the reactor is located in a stainless-steel vessel. Prior to each experiment, the plastic pellets (Fig. 1b) are filled into a 90 mm high container made of graphite foil (Fig. 1c). The container is installed in the reactor so that its base is fixed at the upper end of the isothermal hot zone, as illustrated in Fig. 1d. Additionally, argon adjusts the residence time of the gases in the reactor tube and drives the pyrolysis gases into the sample bag.

2.4. Product analysis

Since during the batch-like experiments no period of stationary gas phase composition can be maintained, all gases leaving the reactor are collected in gas sampling bags during each experiment. Multi-layer film gas sampling bags from Restek with a capacity of 5.0 L are used for this

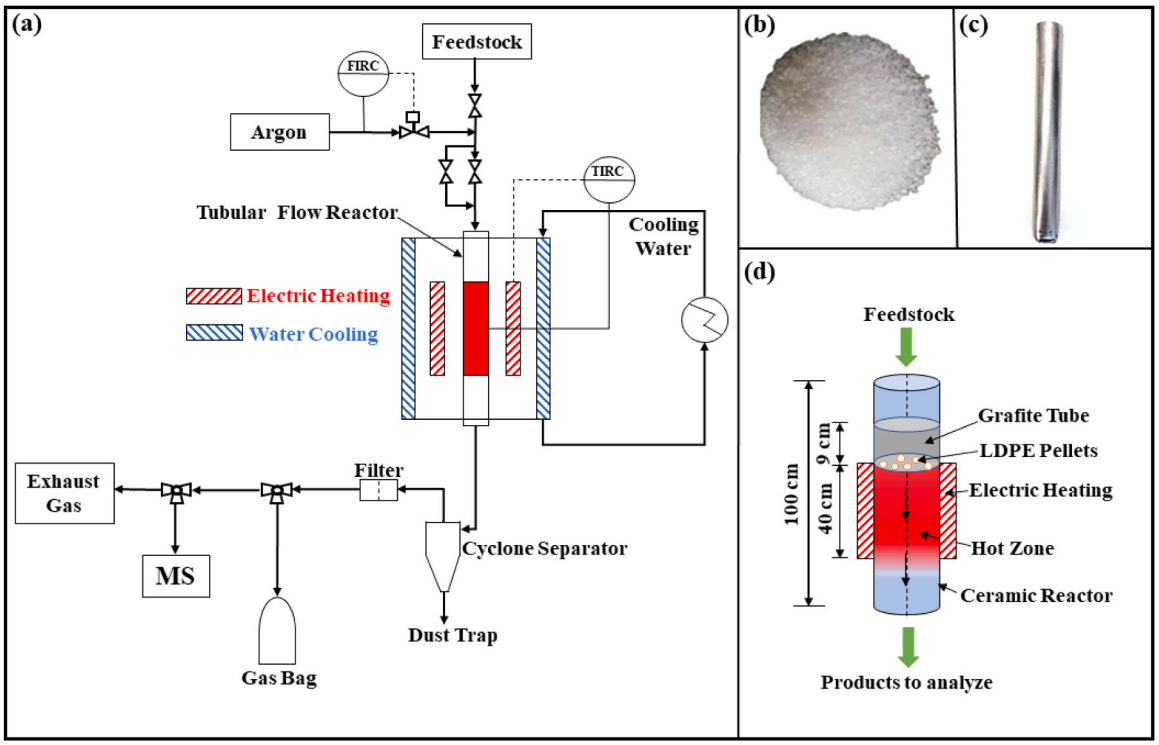

Fig. 1. Flow diagram of the experimental setup (a), plastics pellets (b), graphite tube container (c), and position of the fixed bed container inside the reactor (d).

purpose. An Agilent 6890 gas chromatograph (GC) and a Hiden Analytical HPR-20 R&D mass spectrometer (MS) are used for the subsequent analysis of the gas mixture. The GC is operated with a first-column HAYESEP Q 100/120 column (1 m x 1 mm) and a second-column Shin Carbon ST 100/120 column (2 m x 1 mm) from Restek using helium as the carrier gas. Both columns are utilized in combination to separate the gaseous components (light gases, methane, C_2-, C_3-hydrocarbons) discharged from the reactor. The first column is employed to backflush higher hydrocarbons. The separation is carried out using an oven temperature program that begins at 100 °C for 2 min and then continues with a ramp of 30 °C min^{-1} to up to 300 °C and maintain this temperature for 10 min. Taking into account the time required for the oven to cool down to the initial temperature, the total cycle time for this analysis is less than 19 min. In this way, the species Ar, CH_4, CO, CO_2, C_2H_2, C_2H_4, C_2H_6, C_3H_6 and C_3H_8 are separated and quantified. Each gas sample is analyzed three times using the GC and the final results as presented herein are obtained by averaging. The MS is used to quantify benzene content (C_6H_6). The method used here includes the measuring components Ar, H_2, CH_4, and C_6H_6. The data collected is generated by averaging five measurements. While the GC indicates the absolute concentration of the respective measurement components, the MS normalizes the measured gas components to 100 %. For the gas calibration, we utilized one bottle containing H_2, and C1 to C3 species to calibrate the C1 to C3 range. Another bottle, which contained a mixture of H_2, Ar, and CH_4, was used to calibrate Ar. Additionally, we used a separate bottle of benzene (C_6H_6) in H_2 for calibrating C_6H_6. The GC signals were evaluated by data integration whereas for MS the HIDEN analytical QGA software was used for species quantification with species concentration measured in the range 0.1 ppm to 100 %. The composition of the product stream is calculated from the GC and MS results. The error bar/uncertainty of the GC and the MS were ± 2 % and ± 10 %, respectively.

Regarding the condensable product phase, the samples were collected at the flange of the reactor outlet, the downstream cyclone, the fine filters in the line leading to the analyzers, and the connecting product lines. Subsequently, the soot in all devices was collected and all devices were flushed with hexane, wiped out with filter paper, and thoroughly cleaned by ultrasonic treatment. Afterwards, the soot and the filter papers were extracted in a Soxhlet extractor (period time 4 h) using hexane as solvent.

The Soxhlet extract underwent a solid phase extraction (SPE) treatment to separate aliphatic and aromatic hydrocarbons using UCT Enviro-Clean Fusion Ag^+ sorbent. It consists of silver ions functionalized onto a solid support. Aromatic hydrocarbons are selectively retained on the sorbent by forming a charge-transfer complex with the silver ions. This procedure ensures high capacity for the aromatic hydrocarbons and no breakthrough into the aliphatic fraction. Using the nonpolar solvent hexane, the aliphatics are flushed through the stationary phase without any retention whereas the aromatics are adsorbed. To desorb the aromatics the polar solvent acetone is used. As a result, an aliphatic and an aromatic fraction are obtained which are analyzed by gas chromatography (GC). The gas chromatograph is a ThermoFischer Scientific Trace 1310 GC equipped with a J&W Scientific DB-5 MS column (25 m × 0.32 mm, df = 0.25 μm). The two SPE fractions are injected into the GC and analyzed individually. The components are separated using a temperature program that starts at 40 °C. After 2 min, the temperature ramps up to 120 °C at a rate of 30 °C min^{-1}, followed by a ramp of 8 °C min^{-1} until reaching 330 °C.

In order to determine the yields of the individual species in the gas phase, the MS and GC results were processed as follows: Starting with the averaged results obtained from the three GC measurements, the volume fractions are converted into the yield of the corresponding species. This conversion process involves determining the dosed argon volume over the entire experiment period from the reactor's measurement file. Subsequently, the total volume $V_{T_{gb}}$ of the gas bag is calculated using the volume fraction of argon $y_{A_r}^{GC}$ and the dosed argon volume V_{A_r}, according to Eq. (1). The dosed argon volume was calculated by multiplying the argon gas flow rate by the reaction time. V_{A_r} was 227.13 mL min^{-1}, 205.96 mL min^{-1}, 188.41 mL min^{-1}, 173.61 mL min^{-1}, 160.97 mL min^{-1}, 150.04 mL min^{-1}, 142.90 mL min^{-1}, 132.10 mL min^{-1}, 124.65 mL min^{-1}, and 118.00 mL min^{-1}, for 700 °C, 800 °C, 900 °C, 1000 °C, 1100 °C, 1200 °C, 1300 °C, 1400 °C, 1500 °C, and 1600 °C, respectively, for a residence time of 10 s.

$$V_{T_{gb}} = \frac{V_{A_r}}{y_{A_r}^{GC}} \quad (1)$$

The respective amounts of substance n_j of the species CH_4, CO, CO_2, C_2H_2, C_2H_4, C_2H_6, C_3H_6, and C_3H_8 are calculated using Eq. (2).

$$n_j = y_j^{GC} \frac{pV_{T_{gb}}}{RT} \quad (2)$$

where p is the ambient pressure, R is the ideal gas constant and T is the ambient temperature.

To determine the amount of C_6H_6 produced, the quotient of $y_{C_6H_6}$ and y_{CH_4} is formed with the MS volume fractions. These ratios are calculated with the amount of substance of CH_4, as shown in Eq. (3).

$$n_{C_6H_6} = n_{CH_4} \frac{y_{C_6H_6}^{MS}}{y_{CH_4}^{MS}} \quad (3)$$

The amount of hydrogen is calculated by balancing the amount of analyzed substance. To do this, the sum of the amount of substance of all product gas species n_i is subtracted from the total amount of substance in the sample bag, as seen in Eq. (4).

$$n_{H_2} = \frac{pV_{T_{gb}}}{RT} - \sum n_{\text{iexkl.H}_2} \quad (4)$$

With the initial weight of the polymer $m_{Polymer}$ and the specific molar mass M_i of each species, the yield Y_i per gram of polymer can be calculated using Eq. (5). The fraction of the sum of all gaseous product masses and the polymer mass gives the gas yield.

$$Y_i = \frac{n_i M_i}{m_{Polymer}} \quad Y_{Gas} = \frac{\sum (n_i M_i)}{m_{Polymer}} \quad (5)$$

The combined yield of solid and condensable phases is given by the following relationship from Eq. (6).

$$Rest_{solid+condensed\ phase} = 1 - Y_{Gas} \quad (6)$$

The yields of the individual fractions of the liquid phase were calculated as in Eq. (7). Herein, $m_{i,liq}$ stands for the mass of a specific fraction of the liquid phase, which was determined by GC analysis. More details regarding GC analysis of the liquid sample can be found in Tables S1 and S2 in the SI.

$$Y_{i,liq} = \frac{m_{i,liq}}{m_{Polymer}} \quad (7)$$

The experiments were repeated three times to ensure reproducibility. In this work, the average values are reported in the figures, and the standard deviations of the three repeated runs are used as error bars. The sum of the experimental error bars with regard to gas phase species quantification and carbon balance is less than 5 %.

3. Results and discussion

3.1. Influence of temperature on the gaseous-product composition

Fig. 2 illustrates the results of temperature-dependence tests on LDPE pyrolysis product yields based on MS and GC results, which were conducted in the high-temperature flow reactor described above (Fig. 1). All data were collected at 1 bar pressure using 0.3 g of LDPE pellets for each experiment and a residence time of 10 s concerning the purge gas argon in the hot reactor zone. The yields of gaseous species and non-gaseous species, namely solid carbon as well as condensed phase species, are plotted against the hot zone temperatures. Further details on the impact of temperature on condensed phase products and solid carbon will be provided in Sections 3.2 and 3.3.

The maximum yield in gaseous products of 63.0 wt% is achieved if the LDPE pyrolysis experiment is conducted at a temperature of 800 °C. As the temperature increases, the gas yield gradually decreases to

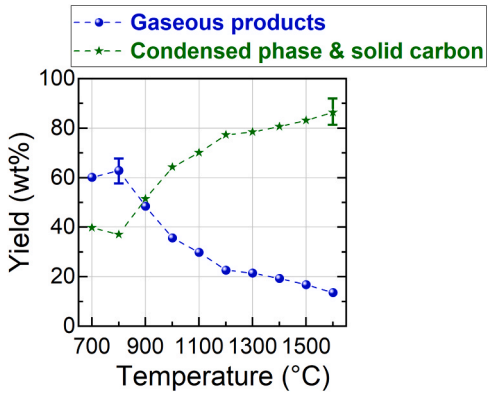

Fig. 2. Temperature influence on mass-related product yields in LDPE pyrolysis.

13.7 wt%. The combined yield of solid carbon and condensed phase species is inversely related. After reaching a plateau between 700 °C and 800 °C, the yield increases to 86.3 wt% at 1600 °C. The minimum value is 37.0 wt% at a temperature of 800 °C.

The yield curves depicted in Fig. 2 can be divided into two regimes. Chemical processes in the temperature range below 900 °C are well-researched and widely understood. As the temperature increases, the endothermic pyrolysis reaction produces smaller primary radicals, which ultimately react to form C_2H_4 through β-cleavage at the polymer chain end [31]. This explains the initial increase in the yield of the pyrolysis gas, as well as the inadequate plastic conversion because plastic droplets were found at 700 °C on the bottom flange at the reactor outlet In the second regime above 900 °C, the dehydrogenation reactions become dominant. As the temperature rises, the composition of the gas phase approaches the thermodynamic equilibrium between H_2 and C, resulting in more carbon being fixed as a solid. Another reason for the higher gas yields at lower temperatures is the gas residence time and the heating rates in the reactor. While the empty tube residence time of argon remains constant throughout the experiments, the residence time of the product gas varies significantly depending on the pyrolysis rate, as the amount of evolving gas governs the total volume and thus the flow rate. In addition, the temperature profile in the hot zone remains constant as shown in Figure S3 (see SI) and also demonstrated in previous studies [32]. During experiments conducted at 1600 °C, there is an immediate and abrupt change in the volume of the gas sample bag after the start of the reaction, whereas during experiments conducted at 700 °C, it is continuously filled. Generally, pyrolysis processes with lower heating rates and longer gas residence times are known to predominantly produce pyrolysis gas, whereas flash pyrolysis processes yield less gas [33]. Williams et al. [21] presented similar results for the pyrolysis of LDPE in a fluidized bed reactor within the lower temperature range. The gas yield increases from 40.1 wt% to 71.4 wt% between 650 °C and 700 °C. Mastral et al. [34] reported the highest gas yield in HDPE pyrolysis at 780 °C, reaching 86.4 wt%. They attribute the decrease in yield with increasing temperatures beyond 850 °C to the growing formation of aromatic hydrocarbons.

In Fig. 3, the gradual increase of carbon black content in the gas phase can be observed as the temperature increases. Between 1100 °C and 1600 °C, black carbon deposits on the lower flange at the outlet of the reactor, whereas at temperatures of 700 °C and 900 °C, shiny brownish substances are visible instead. These substances are likely pyrolysis oils and waxes, which become increasingly dehydrogenated as the temperature rises. The total yield of the condensed phase fraction is around 20.0 wt% and will be discussed later in 3.2. Consequently, this leads to an increase in the production of carbon and hydrogen, as depicted in Figs. 3d and 4.

In Fig. 4a-c, the mole fractions of the measured species are presented as a function of temperature. H_2 is significantly present in the product

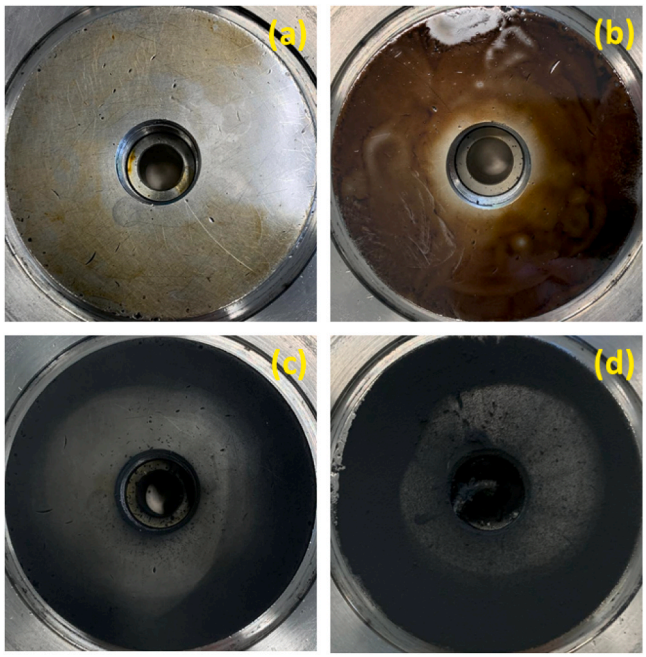

Fig. 3. Flange at the reactor outlet after testing with temperature variation of 700 °C (a), 900 °C (b), 1100 °C (c), and 1600 °C (d).

gas at temperatures about 900 °C. With the increment in temperatures, the mole fraction of H_2 also increases, reaching a value of 98.5 mol% at 1600 °C. On the other hand, the mole fraction of CH_4 in the gas is highest at 900 °C, with a value of 53.7 mol%. The appearance of the deposits at the bottom flange shown in Fig. 4 strongly suggests that the relevance of dehydrogenation reactions increases as the temperature rises. This observation is supported by the data on gas-phase species: While the mole fraction of H_2 in the gas continuously increases (Fig. 4a), other species gradually decompose into solid carbon and hydrogen, particularly at temperatures above 900 °C. Compared to other studies on plastic pyrolysis, qualitatively similar results are achieved in the lower temperature range. For instance, Honus et al. [24,35] reported an increase in the mole fraction of H_2 from 7.7 mol% to 14.2 mol% when the temperature was increased from 700 °C to 900 °C during the pyrolysis of PE. As the temperature reaches 900 °C, the formation of CH_4, C_2H_4, and other alkenes also increases alongside H_2. However, comparing results at temperatures above 900 °C is challenging due to a lack of sufficient research.

Fig. 4d-f depict the mass-related products yield (Eq. 5) as a function of temperature. In contrast, the CH_4 yield steadily increases from 700 °C, reaching a value of 23.2 wt% at 1000 °C. There is no H_2 in the product gas at 700 °C and 800 °C. Starting at 900 °C, the H_2 yield increases to 11.3 wt% at 1600 °C.

When comparing the H_2 yield of 11.3 wt% from the experiment of this work conducted at 1600 °C to the hydrogen mass fraction of about 13.6 wt% present in the LDPE according to Zheng et al. [36], it is evident that a significant portion (around 83.1 wt%) of the hydrogen is released into the gas phase as molecular H_2. The rest remains in the condensed phase and in other hydrocarbon species within the gas phase. The incomplete decomposition into H_2 molecules can be attributed to the sudden increase in volume resulting from the pyrolysis of solid material. This volumetric expansion leads to pressure differentials that facilitate the transport of product molecules in both directions, towards the inlet and the outlet, due to the isotropy of the pressure. Accordingly, gaseous products experience varying residence times based on their direction of movement. Molecules propelled directly towards the outlet of the reactor have shorter residence times compared to those initially directed

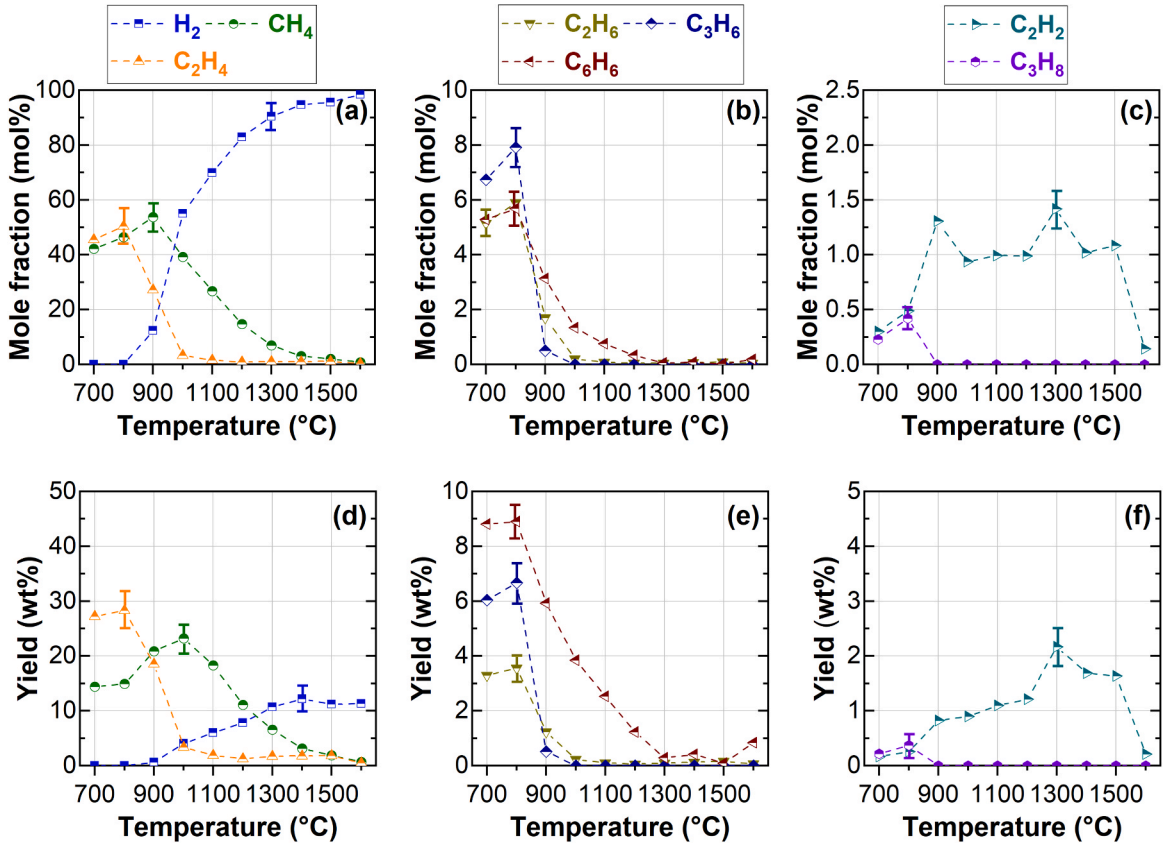

Fig. 4. Temperature influence on the molar gas phase composition (a, b, and c), and on the mass-related product yield during LDPE pyrolysis (d, e, and f).

towards the reactor inlet. The only driving force for their expulsion towards the reactor outlet is the purge gas argon. However, reduced residence times are known to promote the formation of a condensed phase [37], in which additional H atoms are chemically bound in condensed phase hydrocarbons. This observation suggests that, within the reactor configuration employed in this study, the H_2 yield cannot be significantly enhanced by merely increasing the temperature. Instead, a continuous feed of plastic could be implemented to address this challenge, particularly in full-scale applications utilizing a fluidized bed reactor.

Furthermore, experimental results regarding the influence of the argon residence time investigated at 1000 °C can be found in the SI (Figures S4 & S5). Figure S4 depicts that the yield of pyrolysis gas increases as the argon residence time increases (i.e. lower flow rate), rising to a maximum of 55.6 wt% at 20 s. In contrast, the combined yield of solid carbon and condensed phase is inversely proportional, peaking at 79.7 wt% at 3 s. Longer argon residence time allows the product gas to remain in the hot reactor zone longer, facilitating additional secondary reactions. Consequently, at longer argon residence time, there is an enrichment of lighter molecules in the gas phase. According to Figure S5, the H_2 yield increases from 3.3 wt% to 7.5 wt% with longer argon residence. This observation aligns with studies in the pyrolysis of HDPE at 850 °C reported by Mastral et al. [34]. One reason for the decrease in hydrogen yield with increasing argon residence time is that dehydrogenation reactions require longer residence times than random chain breaks and β-cleavages at the chain ends. As the argon residence time decreases (i.e. the argon flow rate increases), the product gas is expelled from the hot reactor zone more rapidly, which cools the environment and inhibits secondary reactions. This explanation is further supported by the observed increase in CH_4, C_2, and C_6H_6 species with lower argon residence time. Additionally, it should be noted that altering the gas residence time at high temperatures (> 1000 °C) significantly affects the interplay between mass transfer and chemical kinetics, hereby also influencing product distributions. For instance, when dehydrogenation reactions are favored to generate hydrogen and carbon, an increasing residence time can hinder the escape of these products, resulting in a higher Damköhler number [38]. This increase can promote further reactions that enhance hydrogen yield. However, as noted by Kim et al. [39] and Tekbas et al. [38], prolonged residence times may also facilitate the occurrence of secondary or undesired reactions, potentially reducing overall process efficiency. This highlights the importance of optimizing reactor conditions to achieve the desired product selectivity and yield.

3.2. *Influence of temperature on condensed phase product species*

Fig. 5 presents the yields of polycyclic aromatics hydrocarbons (PAHs) and aliphatics plotted against the reactor temperature, with Fig. 5a showing yields up to 19.0 wt% and Fig. 5b up to 2.2 wt%.

The yield of aliphatic exhibits a sharp increase from 700 °C to 1000 °C, reaching a maximum of 19.0 wt% at 1000 °C. The yields of PAHs show a similar qualitative trend but at an overall lower level. As the temperature increases, the yield rises from 0.4 wt% at 700 °C to a maximum of 2.2 wt% at 1000 °C.

The increase in the yield of both aliphatic compounds and PAHs increases once again at temperatures exceeding 1400 °C can be attributed to the opposing effect of temperature increase, as detailed in 3.1. The rapid volume change that occurs immediately after loading the reactor with LDPE, in conjunction with rising temperatures, results in decreased residence times for the pyrolysis products within the reactor. While the influence of temperature increase is more pronounced up to 1300 °C, residence time appears to play a more significant role at temperatures above 1400 °C. To minimize the presence of potentially carcinogenic PAHs, it is essential to aim for their complete degradation to carbon during the pyrolysis process [40]. In particular, sufficient residence times and the promotion of deposition reactions have been reported to facilitate carbon formation [41,42]. According to the data presented above (Fig. 4), temperatures of 1300 °C and above are optimal for maximizing the H_2 concentration and yield, exceeding 90.0 mol.% (Fig. 4), while also achieving reasonably low amounts of PAHs (Fig. 5).

Fig. 6 displays the composition of the aliphatic categorized by the number of carbon atoms in the molecule (Eq. 7) and plotted against temperature.

The trend previously discussed in Fig. 5, namely a maximum in yield at 1000 °C and the passing of a local minimum at 1400 °C, is similarly observed in Fig. 6. As depicted in Fig. 6, the yields of short-chain aliphatic below 1000 °C in the condensed phase species can be explained by the high gas output and incomplete conversion of the LDPE (because plastic droplets were found at 700 °C on the bottom flange at the reactor outlet). Between 1000 °C and 1300 °C, the yields of all groups decrease, except for the group with C31-C35. Rising temperatures lead to more random chain breaks, resulting in progressively smaller molecules. The presence of molecules with C36-C40 at 1500 °C and 1600 °C can be explained by the chain length decrease caused by the pyrolysis gases at higher temperatures. Due to the sudden rise in the product gas, the residence time for parts of the condensed phase species in the hot reactor zone is insufficient for splitting. This is also evident from the subsequent increase in yields of molecules with shorter chain lengths from 1500 °C onwards (see Fig. 6a). Fig. 7a&b display the yields of individual groups of PAHs with 2, 3, 4, 5, and 6 rings.

The increase from 700 °C to 1000 °C can be attributed to the temperature-related increase in kinetics towards PAHs. Similar findings were reported by Mastral et al. [34], who observed a reduction in the gas yield during PE pyrolysis due to PAHs formation starting from 850 °C. The formation of PAHs at high temperatures can be explained analogously to their formation during CH_4 pyrolysis. C_2H_4, C_2H_2, and C_3H_6 are considered to be precursors for PAHs. This explains the low PAHs yield observed at 700 °C to 900 °C, as a significant portion of the

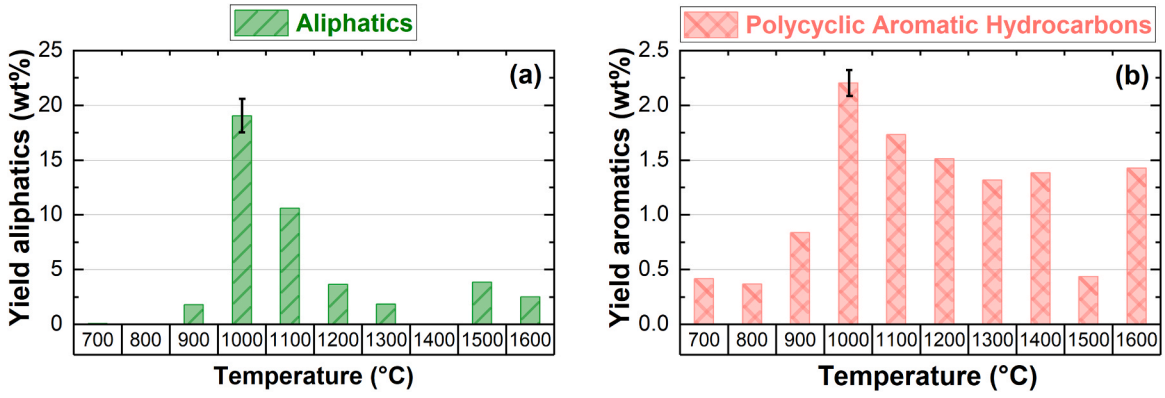

Fig. 5. Temperature influences on the mass-related yield of aliphatics (a) and polycyclic aromatic hydrocarbons (b).

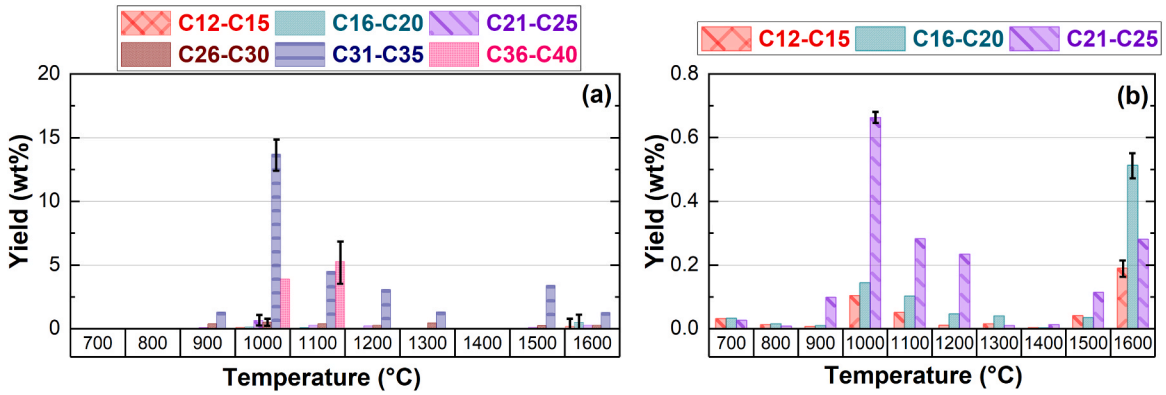

Fig. 6. Temperature influence on the mass yield of grouped aliphatics.

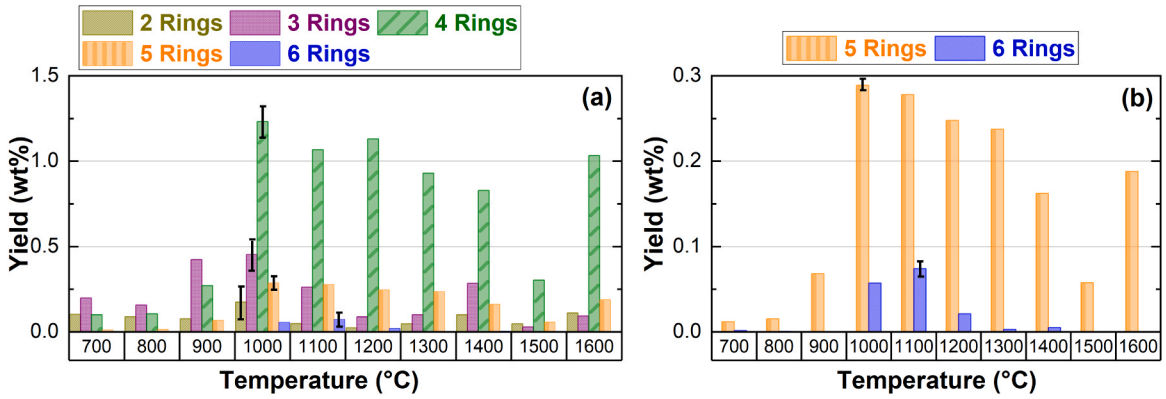

Fig. 7. Temperature influence on the mass yield of PAHs.

precursors remains in the gas phase (28.3 wt% C_2H_4, 0.3 wt% C_2H_2, and 6.7 wt% C_3H_6) and thus only a limited conversion to PAHs takes place. As the temperature increases, more and more C_6H_6 molecules are formed, which according to literature occurs via the dimerization of two propagyl radicals that are formed by the addition of an H radical to C_2H_2 molecules [29,43].

3.3. Influence of temperature on solid carbon

The solid carbon after the pyrolysis of LDPE was also investigated. This data was collected at 1 bar pressure using 15.0 g of LDPE pellets for each experiment and a residence time of 10 s concerning the purge gas argon in the hot reactor zone. A correlation was observed between temperature and the properties of the produced solid carbon.

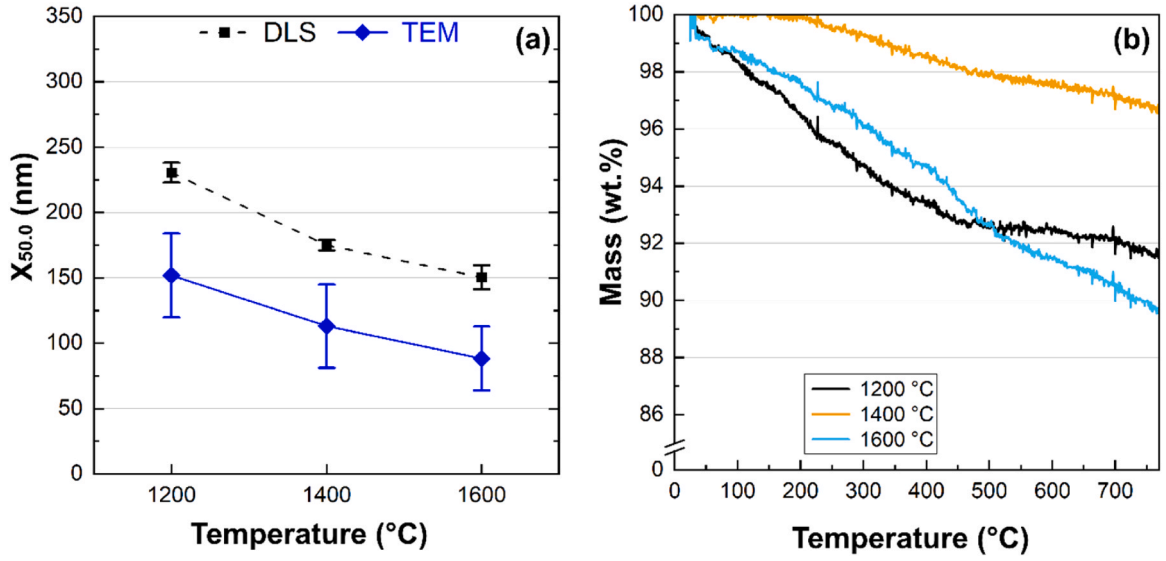

Fig. 8. Number-related median diameter determined by TEM, along with the hydrodynamic median diameter by DLS (a) and the TGA analysis (b) on solid carbon samples from LDPE pyrolysis at reaction temperatures of 1200 °C, 1400 °C and 1600 °C with an argon residence time of 10 s.

Fig. 8 illustrates the relationship between particle sizes and the proportion of volatiles in solid carbon as a function of temperature. As the pyrolysis temperature increases, the size of the primary solid carbon particles decreases as the pyrolysis temperature increases. At 1200 °C, the median particle diameter is 150.0 nm, which significantly decreases to 90.0 nm at 1600 °C. The results from the SEM investigation (Fig. 9) are consistent with the TEM and DLS analyses presented in Fig. 8a. In Fig. 9, the solid carbon exhibits a spherical-like structure with agglomerations of smooth and porous particles. The size of these particles decreases with increasing temperature. This reduction in size is attributed to a higher nucleation rate at higher temperatures, resulting in the formation of a larger number of smaller particles. This phenomenon is observed in LDPE pyrolysis, where higher temperatures shift the thermodynamic equilibrium toward carbon and hydrogen, promoting more uniform nucleation and smaller particle sizes.

TGA analysis (Fig. 8b) reveals that the volatile content of solid carbon varies with temperature. The volatile content reaches a minimum of 3.5 % at 1400 °C, while it increases to 8 % and 10 % at 1200 °C and 1600 °C, respectively. This pattern is likely attributed to the condensation of polycyclic aromatic hydrocarbons (PAHs) and aliphatics on solid carbon particles and reactor surfaces, particularly after the isothermal reactor zone. The decreased volatile content at 1400 °C aligns with findings that this temperature reduces the concentrations of PAHs and aliphatic in the reactor, likely due to optimal reaction kinetics occurring at this intermediate temperature.

The structural properties of solid carbon, as shown in Fig. 10, were analyzed using Raman spectroscopy and X-ray diffraction (XRD). The Raman spectra (Fig. 10a) indicate a decrease in the G/D1 band intensity ratio with increasing temperature, suggesting a lower degree of graphitization in the solid carbon at higher temperatures. XRD analysis further provides insights into the structure; the XRD patterns (Fig. 10b) reveal crystallite structures with interlayer spacings of approximately 4.1 Å. These larger spacings become more pronounced at higher temperatures. The dominant crystallites exhibit a spacing of 3.54 Å for samples collected after experiments conducted at 1200 °C, whereas a reactor temperature of 1600 °C resulted in a significant shift toward the 4.1 Å spacing. The larger spacing of 4.1 Å observed at 1600 °C indicates a disordered arrangement in which carbon layers are misaligned or rotated relative to one another. This misalignment results in wider gaps between the layers that can be attributed to weaker van der Waals interactions. Consequently, this structural arrangement is unique to the pyrolysis of LDPE, as it contrasts with the typical graphite spacing of 3.35–3.5 Å, which is characterized by ordered, stacked graphene layers [44]. Despite these structural changes, the solid carbon remains predominantly amorphous, as evidenced by the broad peaks in the XRD patterns. In summary, the pyrolysis temperature has an insightful impact on the characteristics of solid carbon derived from LDPE pyrolysis. Higher temperatures lead to smaller particle sizes, distinct crystallite structures, and decreased graphitization, providing valuable insights into the mechanisms of solid carbon formation and transformation during plastic pyrolysis. Therefore, the solid carbon produced from LDPE pyrolysis can be compared to industrial thermal black and furnace black of varying quality levels, which are used in elastic rubber applications [45,46].

4. Conclusion

In order to contribute to the development of cost-effective and easily implementable processes for the utilization of plastic wastes, an experimental investigation was conducted on the thermal pyrolysis of plastics. The aim was to examine the influence of different process parameters, in particular temperature on H_2 and solid carbon yield, product gas composition, and condensable hydrocarbon species. Low-density polyethylene (LDPE) served as the feedstock and the effect of temperature was studied using a lab-scale high-temperature tubular flow reactor, which could be loaded with plastic pellets and operated at temperatures ranging from 700 °C to 1600 °C. The results demonstrated that an increase in temperature resulted in a rise in hydrogen yield to over 11 wt% within the temperature range of 900 °C to 1600 °C. Furthermore, the product gas at temperatures of 700 °C to 900 °C mainly consisted of methane and ethylene. This is due to a temperature-related inhibition of hydrogen production in the gas phase. A similar behavior was observed during methane pyrolysis experiments [28,47]. As the temperature increases, the equilibrium of successive dehydrogenation of methane, ethylene, and acetylene tends towards the formation of solid carbon. The study of the temperature's effect on the yields of condensable products revealed that both aliphatic and polycyclic aromatic hydrocarbons (PAHs) increased up to 1000 °C. Aliphatic compounds reached a yield of up to 19.0 wt%, while PAHs yields were approximately an order of magnitude lower throughout the temperature profile. Moreover, the solid carbon produced from the pyrolysis of LDPE was evaluated using analytical techniques such as TEM, SEM, DLS, TGA, XRD and Raman to assess its potential as sustainable industrial carbon material.

In consideration of previous research findings, which revealed a

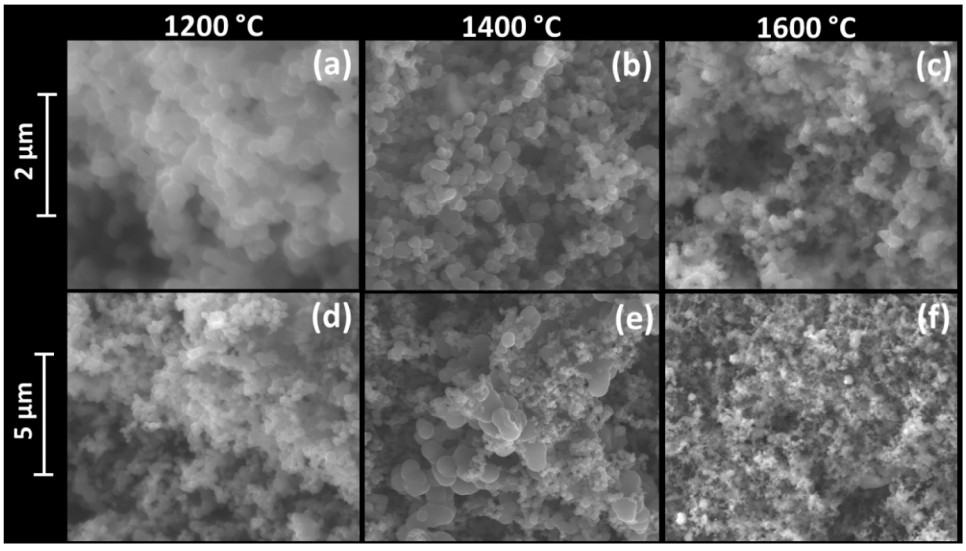

Fig. 9. SEM images on solid carbon samples from LDPE pyrolysis at reaction temperatures of 1200 °C (a, d), 1400 °C (b, e), and 1600 °C (c, f) with an argon residence time of 10 s.

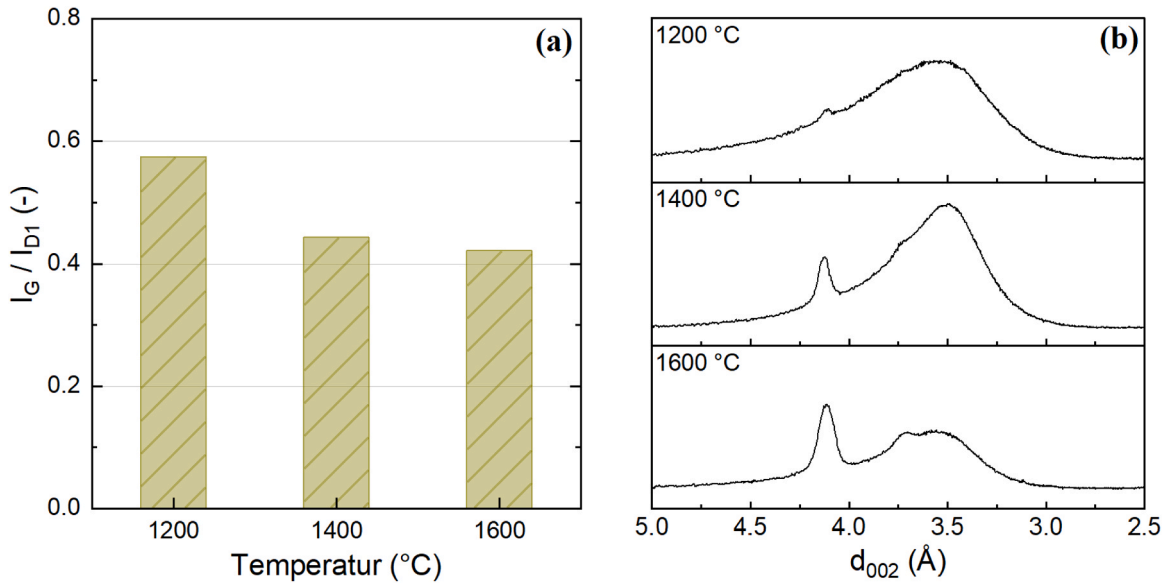

Fig. 10. Intensity ratio of the G- and D1-bands (a), as well as the interlayer spacing d_{002} (b) of the solid carbon samples from LDPE pyrolysis at reaction temperatures of 1200 °C, 1400 °C, and 1600 °C in a fixed bed with an argon residence time of 10 s.

hydrogen production level of $\leq$ 70 mol%) below 900 °C, this work demonstrates that higher temperatures above 900 °C can lead to increased hydrogen yield ($\geq$ 90 mol%). Moreover, it presents the potential to capture carbon black, which could be subsequently utilized by rubber companies. Based on the findings of this study, it is recommended to further investigate the enhancement of hydrogen yield by extending the residence time. Implementing optimized retention of solid and condensed phase products has the potential to result in process improvements in the future (for example the utilization of a batch reactor could allow very high residence time). In summary, the results obtained significantly contribute to our understanding of the thermal pyrolysis of LDPE at temperatures exceeding 1000 °C.

CRediT authorship contribution statement

Cedric Karel Fonzeu Monguen: Writing – review & editing, Writing – original draft, Validation, Methodology, Investigation. **Ahmet Çelik:** Writing – review & editing, Writing – original draft, Validation, Methodology, Investigation. **Felix Straub:** Writing – review & editing, Validation, Investigation, Data curation. **Vanessa Pohl:** Investigation, Data curation. **Jannis Kühn:** Investigation, Data curation. **Patrick Lott:** Writing – review & editing, Validation, Conceptualization. **Olaf Deutschmann:** Writing – review & editing, Supervision, Resources, Conceptualization.

Declaration of Competing Interest

The authors declare that they have no known competing financial interests or personal relationships that could have appeared to influence the work reported in this paper.

Acknowledgements

We thank Berg-idl GmbH for their support in engineering the high-temperature vessel of the experimental setup, and S. Lichtenberg (KIT) for technical support. We are grateful to Dr. Heinz Müller (KIT) for the solid phase extraction (SPE) analysis. We finally acknowledge Dr. Carola Kuhn, Dr. Thomas Jackson Eldrige, Lorena Baumgarten, Shweta Sharma, Andrea Di Giacinto, and Merve Kurt from ITCP (KIT), Daniel Schmider from Eifer, Richard Samman from TVT (KIT), and Dr. Malina Burcea from CVT (KIT) for the characterization of the LDPE pellets and solid carbon samples, as well as the scientific exchange and support.

Appendix A. Supporting information

Supplementary data associated with this article can be found in the online version at doi:10.1016/j.jaap.2025.107289.

Data availability

Data will be made available on request.

References

[1] A.S. Al-Fatesh, N.Y.A. Al-Garadi, A.I. Osman, F.S. Al-Mubaddel, A.A. Ibrahim, W. U. Khan, Y.M. Alanazi, M.M. Alrashed, O.Y. Alothman, From plastic waste pyrolysis to Fuel: Impact of process parameters and material selection on hydrogen production, Fuel 344 (2023) 128107, https://doi.org/10.1016/j.fuel.2023.128107.

[2] M. Sogancioglu, E. Yel, G. Ahmetli, Pyrolysis of waste high density polyethylene (HDPE) and low density polyethylene (LDPE) plastics and production of epoxy composites with their pyrolysis chars, J. Clean. Prod. 165 (2017) 369–381, https://doi.org/10.1016/j.jclepro.2017.07.157.

[3] Z. Hussain, M. Khatak, K.M. Khan, M.Y. Naz, N.M. AbdEl-Salam, K.A. Ibrahim, Production of oil and gas through thermal and thermo-catalytic pyrolysis of waste polyethylene, Mon. Chem. 151 (2020) 1475–1483, https://doi.org/10.1007/s00706-020-02656-9.

[4] F. Riedewald, J. Zuber, P. Rathsack, G. Duffy, M. O'Mahoney, M. Sousa-Gallagher, Chemical recycling of polyolefins with the molten metal reactor at 460 °C, Chem. Ing. Tech. 95 (2023) 1332–1338, https://doi.org/10.1002/cite.202300056.

[5] Relentless O. 2022 Plastic pollution is growing relentlessly as waste management and recycling fall short, says OECD. ⟨Https://www.oecd.org/en/about/news/press-releases/2022/02/plastic-pollution-is-growing-relentlessly-as-waste-management-and-recycling-fall-short.html/⟩, 2022 (accessed on 26 January 2025).

[6] J.N. Hahladakis, C.A. Velis, R. Weber, E. Iacovidou, P. Purnell, An overview of chemical additives present in plastics: Migration, release, fate and environmental impact during their use, disposal and recycling, J. Hazard. Mater. 344 (2018) 179–199, https://doi.org/10.1016/j.jhazmat.2017.10.014.

[7] J.R. Jambeck, R. Geyer, C. Wilcox, T.R. Siegler, M. Perryman, A. Andrady, R. Narayan, K.L. Law, Plastic waste inputs from land into the ocean, Science 347 (2015) 768–771, https://doi.org/10.1126/science.1260352.

[8] K. Ragaert, L. Delva, K. Van Geem, Mechanical and chemical recycling of solid plastic waste, Waste Manag. 69 (2017) 24–58, https://doi.org/10.1016/j.wasman.2017.07.044.

[9] J. Jiang, K. Shi, X. Zhang, K. Yu, H. Zhang, J. He, Y. Ju, J. Liu, From plastic waste to wealth using chemical recycling: a review, J. Environ. Chem. Eng. 10 (2022) 106867, https://doi.org/10.1016/j.jece.2021.106867.

[10] V. Narisetty, R. R, S. Maitra, A. Tarafdar, M.P. Alphy, A.N. Kumar, A. Madhavan, R. Sirohi, M.K. Awasthi, R. Sindhu, S. Varjani and P. Binod, *BioEnerg. Res.* 16 (2023) 16-32. https://doi.org/10.1007/s12155-022-10428-y.

[11] S.H. Gebre, M.G. Sendeku, M. Bahri, Recent trends in the pyrolysis of non-degradable waste plastics, Chem. Open 10 (2021) 1202–1226, https://doi.org/10.1002/open.202100184.
[12] S. Griffiths, B.K. Sovacool, J. Kim, M. Bazilian, J.M. Uratani, Industrial decarbonization via hydrogen: a critical and systematic review of developments, socio-technical systems and policy options, Energy Res. Soc. Sci. 80 (2021) 102208, https://doi.org/10.1016/j.erss.2021.102208.
[13] V.M. Maestre, A. Ortiz, I. Ortiz, Challenges and prospects of renewable hydrogen-based strategies for full decarbonization of stationary power applications, Renew. Sustain. Energy Rev. 152 (2021) 111628.
[14] P. Lott, O. Deutschmann, Heterogeneous chemical reactions—a cornerstone in emission reduction of local pollutants and greenhouse gases, Proc. Combust. Inst. 39 (2023) 3183–3215, https://doi.org/10.1016/j.proci.2022.06.001.
[15] N. Sánchez-Bastardo, R. Schlögl, H. Ruland, Methane pyrolysis for zero-emission hydrogen production: a potential bridge technology from fossil fuels to a renewable and sustainable hydrogen economy, Ind. Eng. Chem. Res. 60 (2021) 11855–11881, https://doi.org/10.1021/acs.iecr.1c01679.
[16] I. Aminu, M.A. Nahil, P.T. Williams, Hydrogen from waste plastics by two-stage pyrolysis/low-temperature plasma catalytic processing, Energy Fuels 34 (2020) 11679–11689, https://doi.org/10.1021/acs.energyfuels.0c02043.
[17] H. Almohamadi, M. Alamoudi, U. Ahmed, R. Shamsuddin, K. Smith, Producing hydrocarbon fuel from the plastic waste: techno-economic analysis, Korean J. Chem. Eng. 38 (2021) 2208–2216, https://doi.org/10.1007/s11814-021-0876-3.
[18] R. Volk, C. Stallkamp, J.J. Steins, S.P. Yogish, R.C. Müller, D. Stapf, F. Schultmann, Techno-economic assessment and comparison of different plastic recycling pathways: a German case study, J. Ind. Ecol. 25 (2021) 1318–1337, https://doi.org/10.1111/jiec.13145.
[19] U. Salahuddin, J. Sun, C. Zhu, M. Wu, B. Zhao, P.-X. Gao, Plastic recycling: a Review on life cycle, methods, misconceptions, and techno-economic analysis, Adv. Sustain. Syst. 7 (2023) 2200471, https://doi.org/10.1002/adsu.202200471.
[20] W. Kaminsky, B. Schlesselmann, C. Simon, Olefins from polyolefins and mixed plastics by pyrolysis, J. Anal. Appl. Pyrolysis 32 (1995) 19–27, https://doi.org/10.1016/0165-2370(94)00830-T.
[21] P.T. Williams, E.A. Williams, Fluidised bed pyrolysis of low density polyethylene to produce petrochemical feedstock, J. Anal. Appl. Pyrolysis 51 (1999) 107–126, https://doi.org/10.1016/S0165-2370(99)00011-X.
[22] B.J. Milne, L.A. Behie, F. Berruti, Recycling of waste plastics by ultrapyrolysis using an internally circulating fluidized bed reactor, J. Anal. Appl. Pyrolysis 51 (1999) 157–166, https://doi.org/10.1016/S0165-2370(99)00014-5.
[23] A. López, I. de Marco, B.M. Caballero, M.F. Laresgoiti, A. Adrados, A. Torres, Pyrolysis of municipal plastic wastes II: Influence of raw material composition under catalytic conditions, Waste Manag 31 (2011) 1973–1983, https://doi.org/10.1016/j.wasman.2011.05.021.
[24] S. Honus, S. Kumagai, G. Fedorko, V. Molnár, T. Yoshioka, Pyrolysis gases produced from individual and mixed PE, PP, PS, PVC, and PET—part I: production and physical properties, Fuel 221 (2018) 346–360, https://doi.org/10.1016/j.fuel.2018.02.074.
[25] M. Sarker, M.M. Rashid, M. Molla, Abundant High-Density Polyethylene (HDPE-2) Turns into Fuel by Using of HZSM-5 Catalyst, J. Fundam. Renew. Energy Appl. 1 (2011) R110201, https://doi.org/10.4303/jfrea/R110201.
[26] Y. Wang, S. Sun, F. Yang, S. Li, J. Wu, J. Liu, S. Zhong, J. Zeng, The effects of activated Al_2O_3 on the recycling of light oil from the catalytic pyrolysis of waste printed circuit boards, Process Saf. Environ. Prot. 98 (2015) 276–284, https://doi.org/10.1016/j.psep.2015.07.007.
[27] M. Cherif Lahimer, N. Ayed, J. Horriche, S. Belgaied, Characterization of plastic packaging additives: food contact, stability and toxicity, Arab. J. Chem. 10 (2017) S1938–S1954, https://doi.org/10.1016/j.arabjc.2013.07.022.
[28] A. Çelik, I. Ben Othman, H. Müller, P. Lott, O. Deutschmann, Pyrolysis of biogas for carbon capture and carbon dioxide-free production of hydrogen, React. Chem. Eng. 9 (2024) 108–118, https://doi.org/10.1039/D3RE00360D.
[29] P. Lott, M.B. Mokashi, H. Müller, D.J. Heitlinger, S. Lichtenberg, A.B. Shirsath, C. Janzer, S. Tischer, L. Maier, O. Deutschmann, Hydrogen production and carbon capture by gas-phase methane pyrolysis: a feasibility study, ChemSusChem 16 (2023) e202201720, https://doi.org/10.1002/cssc.202201720.
[30] S.D. Angeli, S. Gossler, S. Lichtenberg, G. Kass, A.K. Agrawal, M. Valerius, K. P. Kinzel, O. Deutschmann, Reduction of CO_2 emission from off-gases of steel industry by dry reforming of methane, Angew. Chem. Int. Ed. 60 (2021) 11852–11857, https://doi.org/10.1002/anie.202100577.
[31] F.J. Mastral, E. Esperanza, C. Berrueco, M. Juste, J. Ceamanos, Fluidized bed thermal degradation products of HDPE in an inert atmosphere and in air–nitrogen mixtures, J. Anal. Appl. Pyrolysis 70 (2003) 1–17, https://doi.org/10.1016/S0165-2370(02)00068-2.
[32] A. Çelik, A.B. Shirsath, M. Mokashi, J. Tatzig, H. Müller, O. Deutschmann, P. Lott, Climate-friendly hydrogen and carbon production by methane and biogas pyrolysis: Spatial resolution of reactor performance, Chem. Eng. J. 515 (2025) 163167, https://doi.org/10.1016/j.cej.2025.163167.
[33] C.G. Jung, A. Fontana, Production of Gaseous and Liquid Fuels by Pyrolysis and Gasification of Plastics: Technological Approach, Feedstock Recycl. Pyrolysis Waste Plast. Convert. Waste Plast. into Diesel Other Fuels John Wiley Sons Ltd. (2006) 249–283. ISBN: 0-470-02152-7.
[34] F.J. Mastral, E. Esperanza, P. García, M. Juste, Pyrolysis of high-density polyethylene in a fluidised bed reactor. Influence of the temperature and residence time, J. Anal. Appl. Pyrolysis 63 (2002) 1–15, https://doi.org/10.1016/S0165-2370(01)00137-1.
[35] S. Honus, S. Kumagai, V. Molnár, G. Fedorko, T. Yoshioka, Pyrolysis gases produced from individual and mixed PE, PP, PS, PVC, and PET—Part II: Fuel characteristics, Fuel 221 (2018) 361–373, https://doi.org/10.1016/j.fuel.2018.02.075.
[36] Y. Zheng, L. Tao, X. Yang, Y. Huang, C. Liu, Z. Zheng, Study of the thermal behavior, kinetics, and product characterization of biomass and low-density polyethylene co-pyrolysis by thermogravimetric analysis and pyrolysis-GC/MS, J. Anal. Appl. Pyrolysis 133 (2018) 185–197, https://doi.org/10.1016/j.jaap.2018.04.001.
[37] S.D. Anuar Sharuddin, F. Abnisa, W.M.A. Wan Daud, M.K. Aroua, Energy recovery from pyrolysis of plastic waste: study on non-recycled plastics (NRP) data as the real measure of plastic waste, Energy Convers. Manag 148 (2017) 925–934, https://doi.org/10.1016/j.enconman.2017.06.046.
[38] M. Doga Tekbas, M.R. Wright, H.-W. Wong, Primary products from kinetic-limited high-density polyethylene pyrolysis at near vacuum, Chem. Eng. J. 514 (2025) 163347, https://doi.org/10.1016/j.cej.2025.163347.
[39] C.A. Kim, C.A. Sahasrabudhe, Y.-Y. Wang, R. Yappert, A. Heyden, W. Huang, A. D. Sadow, B. Peters, Population balance equations for reactive separation in polymer upcycling, Langmuir 40 (2024) 4096, https://doi.org/10.1021/acs.langmuir.3c03004.
[40] K. Hussain, R.R. Hoque, S. Balachandran, S. Medhi, M.G. Idris, M. Rahman, F. L. Hussain, Monitoring and risk analysis of PAHs in the environment, in: C. M. Hussain (Ed.), Handbook environm. mater. manag. Springer International Publishing AG, 2018, pp. 1–35, https://doi.org/10.1007/978-3-319-58538-3_29-2.
[41] S.V. Papuga, P.M. Gvero, L.M. Vukić, Temperature and time influence on the waste plastics pyrolysis in the fixed bed reactor, Therm. Sci. 20 (2016) 731–741, https://doi.org/10.2298/TSCI141113154P.
[42] J.A. Onwudili, N. Insura, P.T. Williams, Composition of products from the pyrolysis of polyethylene and polystyrene in a closed batch reactor: effects of temperature and residence time, J. Anal. Appl. Pyrolysis 86 (2009) 293–303, https://doi.org/10.1016/j.jaap.2009.07.008.
[43] M. Mokashi, A.B. Shirsath, A. Çelik, P. Lott, H. Müller, S. Tischer, L. Maier, J. Bode, D. Schlereth, F. Scheiff, D. Flick, M. Bender, K. Ehrhardt, O. Deutschmann, Chem. Eng. J. 485 (2024) 149684, https://doi.org/10.1016/j.cej.2024.149684.
[44] E. Olsson, J. Cottom, H. Au, Z. Guo, A.C.S. Jensen, H. Alptekin, A.J. Drew, M.-M. Titirici, Q. Cai, Elucidating the effect of planar graphitic layers and cylindrical pores on the storage and diffusion of Li, Na, and K in carbon materials, Adv. Funct. Mater. 30 (2020) 1908209, https://doi.org/10.1002/adfm.201908209.
[45] Y. Fan, G.D. Fowler, M. Zhao, The past, present and future of carbon black as a rubber reinforcing filler – a review, J. Clean. Prod. 247 (2020) 119115, https://doi.org/10.1016/j.jclepro.2019.119115.
[46] L. Moulin, S. Da Silva, A. Bounaceur, M. Herblot, Y. Soudais, Assessment of recovered carbon black obtained by waste tires steam water thermolysis: an industrial application, Waste Biomass Valor. 8 (2017) 2757–2770, https://doi.org/10.1007/s12649-016-9822-8.
[47] M. Mokashi, A. Bhimrao Shirsath, P. Lott, H. Müller, S. Tischer, L. Maier, O. Deutschmann, Understanding of gas-phase methane pyrolysis towards hydrogen and solid carbon with detailed kinetic simulations and experiments, Chem. Eng. J. 479 (2024) 147556, https://doi.org/10.1016/j.cej.2023.147556.